Proc. Estonian Acad. Sci. Eng., 2000, **6**, 4, 259–267
https://doi.org/10.3176/eng.2000.4.01

PIANO HAMMER TESTING DEVICE

Anatoli STULOV[a] and Avo MÄGI[b]

[a] Institute of Cybernetics, Tallinn Technical University, Akadeemia tee 21, 12618 Tallinn, Estonia; stulov@ioc.ee
[b] Tallinn Piano Factory, Kungla 41, 10413 Tallinn, Estonia; hiis@online.ee

Received 5 June 2000

Abstract. The piano hammer testing device described here makes it possible to investigate the dynamic force–compression characteristics of the piano hammer and, using the hereditary (hysteretic) hammer model, to find the hammer parameters by numerical simulation of the dynamic experiments.

Key words: grand piano, piano hammer, hammer model, hammer–string interaction.

1. INTRODUCTION

According to the hammer models considered earlier, the loading and unloading of the hammer are reversible. Usual model of the hammer relates the force exerted by hammer F and the hammer felt compression u in the form of the power law [1–4]

$$F = F_0 u^p , \tag{1}$$

where F_0 is the hammer stiffness and p is the compliance nonlinearity exponent. Thus the features of the hammer are determined by these two parameters which may be easily measured in static experiments. However, dynamic features of piano hammers are significantly more complicated.

The results of the experiment provided by Yanagisawa, Nakamura, and Aiko [5,6] show significant influence of the hysteresis, i.e., loading and unloading of the hammer are not alike. Furthermore, the force–compression relationships of the hammer are essentially nonlinear and the slope of the dynamic force–compression curve is strongly dependent on the hammer velocity. The model of the hammer that takes into account all the dynamic features of the hammer and uses real hammer

parameters that are independent of the hammer velocity was derived in [7] in the form

$$F(u(t)) = F_0 \left[u^p(t) - \frac{\varepsilon}{\tau_0} \int_0^t u^p(\xi) \exp\left(\frac{\xi - t}{\tau_0}\right) \mathrm{d}\xi \right]. \tag{2}$$

According to this model, the real piano hammer possesses history-dependent properties or, in other words, is made of a material with memory. Two additional hereditary parameters, hereditary amplitude ε and relaxation time τ_0, are used to describe the hysteretic behaviour of the hammer.

Suitable values of elastic parameters F_0, p and hereditary constants ε and τ_0 for various hammers may be obtained by numerical simulation of the dynamic experiments. The mathematical model of the experiment presented below can be described as

$$m\frac{\mathrm{d}^2u}{\mathrm{d}t^2} + F(u) = 0, \tag{3}$$

with initial conditions

$$u(0) = 0, \quad \frac{\mathrm{d}u}{\mathrm{d}t}(0) = V_0. \tag{4}$$

Here m and V_0 are the hammer mass and velocity.

2. EXPERIMENTAL ARRANGEMENT

The experimental arrangement shown in Fig. 1 gives a possibility to obtain the dynamic force–compression characteristics of piano hammers and, using the hereditary model of the hammer (Eq. (2)), to find the hammer parameters by numerical simulation of the dynamic experiments.

In the measurements the hammer struck a piece of the string, fixed on the force sensor. The device consists of two main parts. The first part gives the needed velocity of interaction of the hammer with the string. The second part includes the force and gap sensors with respective electronics for the registration of the force–time and compression–time dependences during the strike.

General view of the device is shown in Fig. 2. A piezoelectric wide-band ceramic plate is used as a force sensor. To measure the hammer compression, an infrared optical system has been developed. During the strike, the flag placed on the end of the shank changes the intensity of the infrared light between the emitter and receiver diodes that gives the possibility to measure the hammer felt compression. To avoid the influence of the shank deformation, it is made of a rigid titanium tube.

The mass of the shank M_s is equal to 13.5 g, and the mass of the hammer holding unit M_u to 33 g. Thus the effective mass that is added to the hammer mass during the numerical simulation of the experiment is equal to $M_\mathrm{a} = 1/3\ M_\mathrm{s} + M_\mathrm{u} =$ 37.5 g.

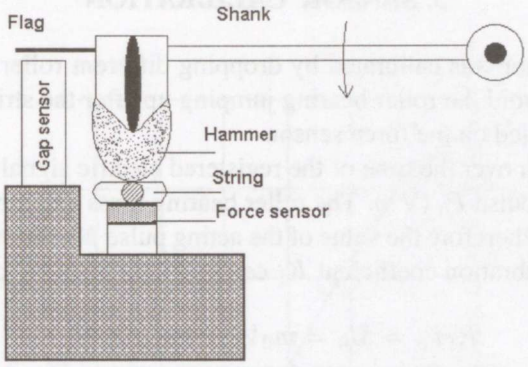

Fig. 1. Experimental arrangement for dynamic testing of piano hammers.

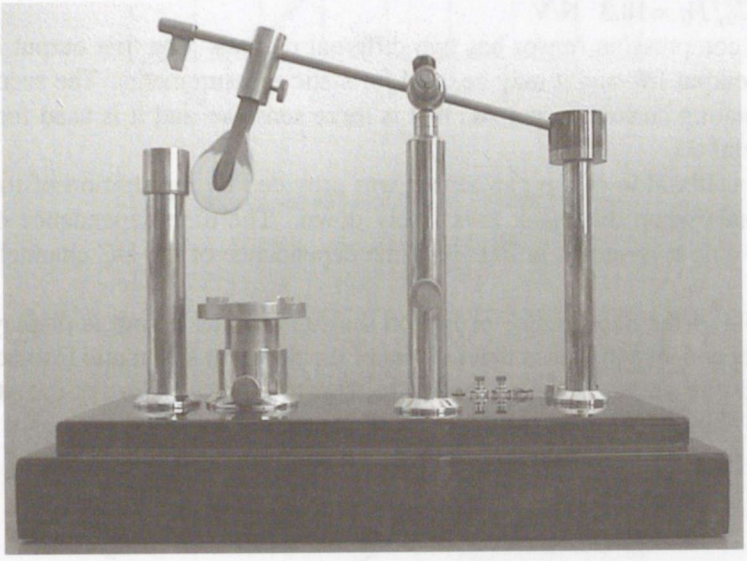

Fig. 2. Piano hammer testing device.

The analogue signals from the force and the gap sensors are converted into two sets of data by a digital signal processor ADSP-2181. This 8-channel 12-bit processor allows:

– to set up the data communication speed from the device sensors to the computer,

– to present data in the scope mode or in the analyser (FFT) mode,

– to save data in a file,

– to print oscillograms and spectrograms.

The device is controlled by a personal computer via a RS232 cable.

3. SENSOR CALIBRATION

The force sensor was calibrated by dropping different roller bearings onto the force sensor. To avoid the roller bearing jumping up after the strike, a piece of thin sticky tape was glued on the force sensor.

The integration over the time of the registered electric signal gives the value of the roller bearing pulse P_0 (V s). The roller bearing mass and the dropping altitude are known values, therefore the value of the acting pulse M_0 (kg m/s) is also known. Thus the force calibration coefficient K_f can be found from the equation

$$K_\mathrm{f} P_0 = M_0 = m_0 V_0 = m_0 \sqrt{2gH_0}. \tag{5}$$

Here m_0, V_0, and H_0 are the roller bearing mass, velocity, and the amplitude of falling and g is the gravity constant. The value of the calibration coefficient was found by averaging the results of a series of measurements and it is equal to $K_\mathrm{f} = M_0/P_0 = 18.3$ N/V.

The compression sensor has two different outputs. The first output is a direct current output DC and it may be used for static measurements. The second one is an alternating current output AC that is more sensitive and it is used for dynamic measurements.

The calibration of the gap sensor was provided by registration of the AC and DC signals when the shank falls freely down. The time dependence of the AC channel output is shown in Fig. 3. Time dependence of the DC channel output is similar.

In Fig. 4 the dependence of DC on the AC channel output is displayed. This linear dependence indicates that in spite of the different schematic formation of the channels they are functioning identically. Thus we may be sure that the AC channel is broad enough to reproduce the form of the signal.

The linear dependence shown in Fig. 4 may be approximated as

$$U_\mathrm{dc} = 4.473 + 0.1005\, U_\mathrm{ac}. \tag{6}$$

This function relates the output voltages of DC and AC channels.

From Fig. 3 we find that the optical aperture is slightly closed if the output voltage in AC channel exceeds 0.0815 V. If the output voltage in AC channel exceeds 4.710 V, then the optical aperture is closed completely. The diameter of the working aperture D_a (the maximum value of hammer felt compression) was found by using a micrometer. It is equal to 2.0 mm.

While falling down for such a small distance, the force of gravity changes the shank velocity V_a just a little. Therefore we may assume that during the measurement the velocity V_a is constant. In this case we have

$$V_\mathrm{a} = D_\mathrm{a}/t_\mathrm{a} = 1.52 \ \mathrm{m/s}, \tag{7}$$

where t_a = 1.316 ms is the falling time obtained from Fig. 3.

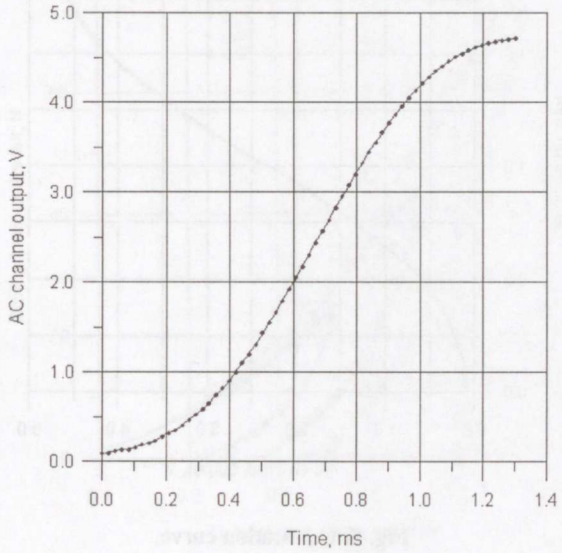

Fig. 3. Time dependence of the AC channel output.

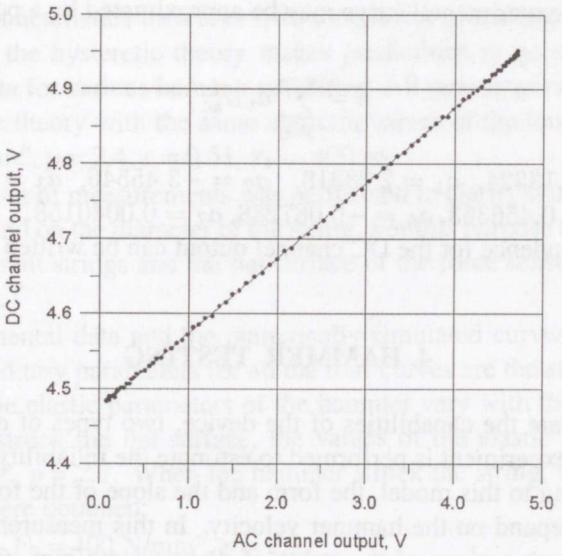

Fig. 4. Dependence of DC on AC channel output.

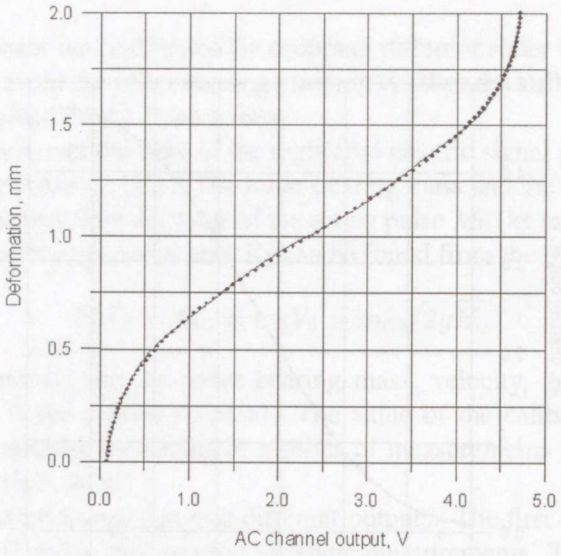

Fig. 5. Calibration curve.

Because the displacement of the flag through the optical aperture is proportional to time, using Eq. (7) we may replace the time axis in Fig. 3 by displacement axis (hammer compression). This calibration curve is presented in Fig. 5. For numerical calculations this experimental curve may be approximated by a polynomial

$$u = \sum_{i=0}^{7} a_i U_{\text{ac}}^i , \tag{8}$$

where $a_0 = -0.13324$, $a_1 = 2.28318$, $a_2 = -3.45546$, $a_3 = 3.15284$, $a_4 = -1.60758$, $a_5 = 0.456363$, $a_6 = -0.067288$, $a_7 = 0.0040158$.

Similar dependence for the DC channel output can be written using Eq. (6).

4. HAMMER TESTING

To demonstrate the capabilities of the device, two types of experiments were made. The first experiment is performed to estimate the reliability of the hysteretic model. According to this model, the form and the slope of the force–compression characteristics depend on the hammer velocity. In this measurement the hammer (*Renner* A1) struck a piece of the string of diameter 4.3 mm, fixed on the force sensor, and the force–compression relationships for various hammer velocities were obtained.

A comparison of the theoretical model with the experimental data is presented in Fig. 6. Experiment confirms the theory fairly well. The slope of the force–

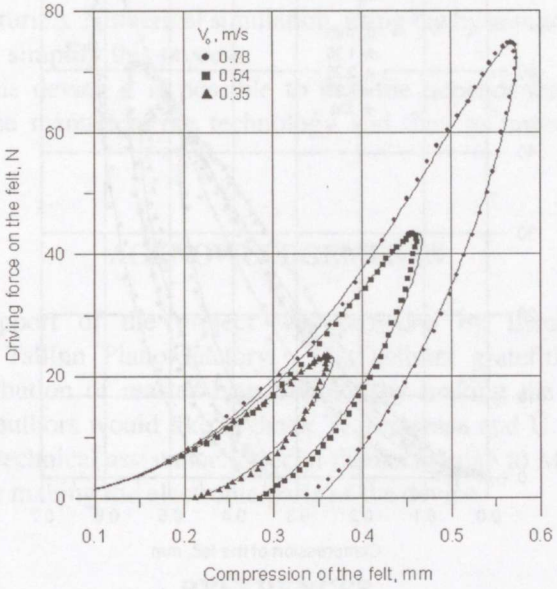

Fig. 6. Experimentally obtained force–compression characteristics of the *Renner A*1 hammer for various initial velocities V_0 of the hammer; solid lines are calculated curves.

compression characteristics increases with the growth of the hammer velocity. On the other hand, the hysteretic theory makes predictions in good agreement with experimental data for various hammer velocities. All three experimental curves are described by the theory with the same constant values of the hammer parameters: $F_0 = 400$ N/mm^p, $p = 2.4$, $\varepsilon = 0.51$, $\tau_0 = 400$ μs.

The second set of measurements was performed to clarify whether the hammer parameters depend on the diameter of the string. For this purpose the hammer (*Abel* A1) struck different strings and the flat surface of the force sensor with a constant velocity 0.7 m/s.

The experimental data and the numerically simulated curves are presented in Fig. 7. The hereditary parameters for all the four curves are the same: $\varepsilon = 0.69$ and $\tau_0 = 250$ μs. The elastic parameters of the hammer vary with the string diameter. If the hammer struck the flat surface, the values of the elastic parameters were: $F_0 = 480$ N/mm^p, $p = 2.7$. When the hammer struck the string, the following sets of parameters were obtained:

$d = 4.3$ mm: $F_0 = 400$ N/mm^p, $p = 2.3$,

$d = 2.25$ mm: $F_0 = 330$ N/mm^p, $p = 2.0$,

$d = 1.25$ mm: $F_0 = 270$ N/mm^p, $p = 1.8$.

Thus the hammer parameters strongly depend on the string diameter or on the conditions of interaction.

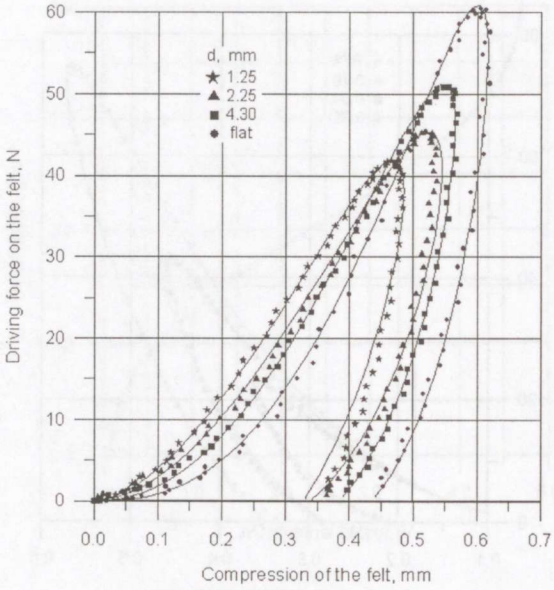

Fig. 7. Experimentally obtained force–compression characteristics of the *Abel A*1 hammer striking various strings and the flat surface; solid lines are calculated curves.

5. CONCLUSIONS

To measure the nonlinear elastic and hereditary parameters of the piano hammer, a special device has been developed. This experimental arrangement gives the possibility to investigate the dynamic force–compression characteristics of the piano hammer and, using the hereditary (hysteretic) hammer model [7], to find the hammer parameters by numerical simulation of the dynamic experiments.

It has been shown that physical assumptions about the history-dependent properties of the hammer felt are confirmed by the experiments. The hereditary model of the hammer with memory describes the behaviour of such microstructured material as hammer felt rather well. The dependence of the slope of the force–compression characteristics of the hammer on the rate of loading is obvious (Fig. 6).

The model demonstrated here makes predictions in good agreement with experimental data for various types of piano hammers and for a broad range of hammer velocities. This model makes it possible to find the additional intrinsic (hereditary) parameters of the hammer.

It has been shown that the values of the hammer parameters depend on the diameter of the struck string (Fig. 7).

The piano hammer testing device in conjunction with the hysteretic model of the hammer is a powerful instrument for matching of the piano hammers, as well as for their manufacturing. Numerical simulation, using the hysteretic hammer model, may significantly simplify this process.

By use of this device it is possible to find the dependence of the hammer parameters on the manufacturing technology and thus to improve the hammer quality.

ACKNOWLEDGEMENTS

Financial support of the project was provided by Estonian Innovation Foundation and Tallinn Piano Factory. The authors gratefully acknowledge significant contribution of master Ivan Sokolov by making the brass details of the device. The authors would like to thank T. Terasmaa and Ü. Kuusk for their engineering and technical assistance. Special thanks are due to M. Sidorenko and ADIMIR Ltd. for making the electronic parts of the device.

REFERENCES

1. Ghosh, M. An experimental study of the duration of contact of an elastic hammer striking a damped pianoforte string. *Indian J. Phys.*, 1932, **7**, 365–382.
2. Hall, D. E. and Askenfelt, A. Piano string excitation. V. Spectra for real hammers and strings. *J. Acoust. Soc. Am.*, 1988, **83**, 4, 1627–1638.
3. Russell, D. and Rossing, T. Testing the nonlinearity of piano hammers using residual shock spectra. *Acustica*, 1998, **84**, 967–975.
4. Giordano, N. and Winans II, J. P. Piano hammers and their force compression characteristics: Does a power law make sense? *J. Acoust. Soc. Am.*, 2000, **107**, 4, 2248–2255.
5. Yanagisawa, T., Nakamura, K., and Aiko, H. Experimental study on force–time curve during the contact between hammer and piano string. *J. Acoust. Soc. Jpn.*, 1981, **37**, 1, 627–633.
6. Yanagisawa, T. and Nakamura, K. Dynamic compression characteristics of piano hammer felt. *J. Acoust. Soc. Jpn.*, 1984, **40**, 11, 725–729.
7. Stulov, A. Hysteretic model of the grand piano hammer felt. *J. Acoust. Soc. Am.*, 1995, **97**, 4, 2577–2585.

KLAVERI HAAMRI KATSETAMISE SEADE

Anatoli STULOV ja Avo MÄGI

On kirjeldatud seadet, mille abil saab uurida klaveri haamri töö füüsikalisi protsesse. Haamri hüstereesilisel mudelil põhinev seade ja selle tarkvara võimaldavad modelleerida helitekkeprotsessi ja ennustada klaveri kvaliteeti.